SUPPORTING INFORMATION:

Hybrid Metal-Dielectric Zero Mode Waveguide for Enhanced Single Molecule Detection

Xavier Zambrana-Puyalto,[a] Paolo Ponzellini,[a] Nicolò Maccaferri[b], Enrico Tessarolo,[c] Maria G. Pelizzo,[c] Weidong Zhang,[d] Grégory Barbillon,[e] Guowei Lu,[d] and Denis Garoli[a*]*

[a] Istituto Italiano di Tecnologia – Via Morego, 30, I-16163 Genova, Italy
[b] Physics and Materials Science Research Unit, University of Luxembourg, L-1511 Luxembourg, Luxembourg
[c] CNR-IFN, Via Trasea 7, Padova (Italy)
[d] State Key Laboratory for Mesoscopic Physics & Collaborative Innovation Center of Quantum Matter, School of Physics, Peking University, Beijing 100871, China
[e] EPF—École d'Ingénieurs, 3 bis rue Lakanal, 92330 Sceaux, France
[*] Corresponding author's email: denis.garoli@iit.it, xavier.zambrana@iit.it

Supporting note #1 – Samples fabrication

150 μm thick glass slides have been used as the substrate. Firstly, the substrates have been thoroughly cleaned in order to obtain a smooth metallic surface with the subsequent metal deposition. The substrates have been washed in a piranha solution (3:2 H_2SO_4:H_2O_2), thoroughly rinsed in deionized water, and subsequently sonicated in acetone and in isopropanol. The substrates have been dried by means of a nitrogen gun. The metal layers, then have been deposited by means of electron-beam evaporation in high-vacuum. The use of a thin layer of titanium is typically required in order to avoid the detachement of the metallic layers from glass, but in this experiment we observed that silicon itself acts as a good adhesion layer between gold and glass. Hence, for the hybrid Si-Au nanoslots, a 20 nm silicon layer has been evaporated directly on the glass substrate, at a deposition rate of 1 Å/s, and a 80 nm layer of gold has been evaporated above the silicon layer, at the rate of 0.3 Å/s, without breaking the vacuum in the vacuum chamber, between the two depositions.

The bilayer has been drilled by means of a gallium FIB at an accelerating bias of 30 kV, with a dwell time of 1 μs, and with the ionic current set to a low value (24 pA) in order to obtain a tiny beam and hence narrow structures. 100x100 μm^2 arrays of nanoslots with inter-distance between 2 and 5 μm have been prepared in few seconds of exposure (To note that higher density of nanoslots can be achieved changing the pattern parameters). Worth to note, it has been demonstrated that Ga implantation during FIB fabrication can change the optical properties of plasmonic nanostructures (see for instance Ref.[1s]). However, as demonstrated in some recent works[2s,3s], the effect on the optical

response and on the near-field enhancement in the near-IR, which is the spectral range explored in our experiments, is pretty negligible[3s].

Due to the high aspect ratio of our structures, the actual inner shape of the nanoslots is not visible by means of a top view SEM image. Only the upper, external shape of the nanoslots, at the gold-water interface, results clearly visible and measurable. For evaluating the milling parameters, both in the vertical and horizontal planes, several cross-sections have been realized on trial nanoslots. First of all, this approach has allowed us to calibrate the milling time, in order to reach the glass substrate below the metallic layer, without digging into the glass. In the second place, it has allowed us to measure the resulting slope of the nanoslot walls. This way we could calibrate the design of the nanoslots within the FIB software in order to obtain the desired rectangular shape with the optimal simulated dimensions (35x100nm^2), at the nanoslot bottom interface.

The gold nanoslots (Fig. S1) have been fabricated with the same procedure, with the obvious exception of the material deposition. Even in this case the deposition was performed in an electron beam evaporator, in high vacuum. But here a 3nm thick titanium layer has been used as the linker. Titanium has been deposited at 0.3 Å/s. Above the titanium layer, a 100 nm gold layer has been deposited, still at 0.3 Å/s, without breaking the vacuum, between the two depositions.

Noteworthy, the used fabrication procedure can also enable to prepare over-drilled ZMWs where also the glass substrate is partially milled. In particular, over-drilled ZMWs have been demonstrated to produce additional enhancement in fluorescence emission[4s-6s].

Once fabricated, the samples have been stored in a nitrogen atmosphere to avoid deterioration. Before the fluorescence measurements, a 90 seconds oxygen plasma (100% O_2; 100 W) was performed on the sample. The plasma treatment is fundamental to make the surface hydrophilic, and hence to ensure that water enters the nanoantennas.

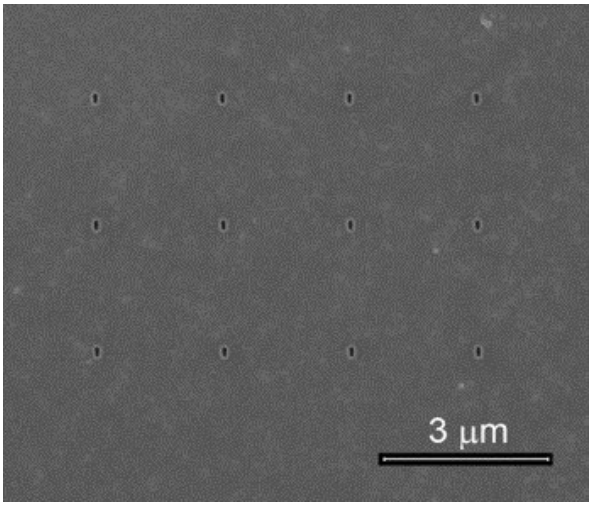

Figure S1. Example of Au nanoantennas.

Supporting Note #2 - Numerical Simulations

Numerical simulations based on the finite element method implemented in Comsol Multiphysics were carried out to investigate the electromagnetic response of an isolated plasmonic ZMW. The dimensions of the simulated ZMWs were set according to the average sizes obtained from SEM investigations. A dielectric constant n = 1.33 was used for water, and n = 1.5 was set for the glass substrate. The model computes the electromagnetic field in each point of the simulation region, enabling the extraction of the quantities plotted along the manuscript. The unit cell was set to be 250 nm wide in both *x*- and *y*-directions and 1000 nm along the z-direction, with perfect matching layers (150 nm thick) at the borders. Either a Gaussian beam or a linearly polarized plane wave impinges on the structure from the glass side, with the electric field aligned along the short axis of the ZMW.

Supporting Note #3 - Optical set-up

The experiments are performed on an inverted microscope with an oil-immersion (NA=1.3) microscope objective. The light beam, which enters the microscope through its rear port, is obtained with a supercontinuum laser (with a repetition rate of 80MHz), which has been previously coupled to a single mode fiber. The polarization of the beam coming out of the single mode fiber is linearly polarized, but we have not implemented any sort of polarization control afterwards. Hence, the polarization at the focal plane is elliptically polarized. Three different central wavelengths have been used: 587, 633, and 676 nm. The linewidths of each case are 15, 17, 20 nm, respectively. All the experiments have been performed at a power of 25 μW. The samples that we used for the experiment are held on a sample holder, which is attached to a micro and a nanopositioner. The nanopositioner is used to center the sample with respect to the incident beam. The nanopositioner is also used to place the sample at the z-plane where the fluorescence counts are maximized. All the samples are cleaned with an oxygen plasma at 100 W for 2 min before being used. For each of the wavelengths, a different dye of the Alexa family is used: Alexa610, Alexa647 and Alexa680. For the three cases, a 30 μL droplet of the corresponding solution of dyes is used. The concentration is always kept at 50 μg/mL for the experiments with the ZMWs. The confocal experiments have been done with two different concentrations, 10 ng/mL and 100 ng/mL. Three filters are used to separate the fluorescence of the dyes from the light reflected off the sample. The filters are a dichroic mirror (DM), and a combination of either two bandpass filters (BP) or a longpass filter (LP) and a BP. For Alexa610, the filters were: DM at 594 nm, a LP at 633 nm, and a BP at 641/75 nm. For Alexa647: DM notch at 633 nm, and two BPs at 698/70 nm and at 680/42 nm. For Alexa680: DM at 685 nm, a LP at 685 nm and a BP at 711/25 nm. After the last BP filter, a 50/50 beam splitter is used to split the fluorescence light signal into two different channels. Then, two 50 mm lenses are used to focus the fluorescence signal

onto two equivalent avalanche photodiodes (APD). The APDs are re-aligned with XY translation stages for each different wavelength. The signal of the APDs is recorded with a time-correlated single photon counting module. (To note that the 50μm chip of the APD is used as a pinhole).

Our optical set-up can resolve an average number of molecules that ranges from 0.05 to 50000 doing FCS measurements. The higher limit is given by the noise in the correlation function $G(\tau) = \langle F(t)F(t+\tau)\rangle/\langle F(t)\rangle^2$, where F(t) is the fluorescence signal, τ is the lag time and $\langle\rangle$ indicates time averaging. 50000 molecules yield a correlation value that is equivalent to the correlation value of the background noise. In contrast, the lower noise is given by the absence of fluorescence counts in the time span of the correlation function. Now, the number of molecules is proportional to the concentration, but it is also affected by the detection volume of the structure. Thus, each structure works for a specific range of concentrations such that the number of molecules is in between 0.05 and 50000.

Supporting Note #4 - FCS measurements

The fluorescence trace duration is typically 1 minute. The binning time has been maintained between 10 and 200 ns, depending on the case. After the detection of the fluorescence trace, three different calculations are carried out to be able to retrieve the count rate per molecule (CRM). First, the signals measured by the two APDs are correlated. A 2D translational diffusion model is used to fit the correlation function and obtain the average number of molecules $\langle N\rangle$[7s]. This is a valid approximation of a 3D diffusion model when of the axial size of the observation volume is much larger than its lateral[8s]. Second, the average of the fluorescence trace $\langle F\rangle$ and its standard deviation δF are calculated. Finally, the CRM is obtained as $CRM = \langle F\rangle/\langle N\rangle \pm \delta F/\langle N\rangle$. This operation is performed several times, and the final CRM is obtained as an average of the different CRM measurements for each slot.

The definition of fluorescence enhancement (FE) is done as the CRM for the nanoslot divided over the CRM for the confocal case. A detailed description of the calculation is reported in Ponzellini et al 2018 (main text ref.[17]). In particular, the FE of a nanoslot (ZWM) were obtained as $FE = CRM_{ZMW}/CRM_{conf}$.

The volume reduction is computed as a ratio of the detection volume of the nanoslot (ZMW) over the detection volume of the confocal case. A detailed description of the calculation is reported in[17]. In particular, the VR of a nanoslot (ZWM) were obtained as $VR = DV_{Conv}/DV_{ZMW}$, where the detection volume is DV = N/C, where N is the number of molecules and C the concentration.

Supporting Note #5 - Lifetime measurements

The APDs as well as the laser are connected to a time-correlated single-photon counting module in time-resolved mode. Making use of a home-built code, we build a histogram of 300 bins, each of them having a temporal width of 30 ps. A certain time delay is applied to the laser channel, so that the histogram is monotonously decreasing. The histogram measurement is carried out for 150 s. A single exponential $Te^{-t/\tau}$ is used to fit the confocal histograms, whereas biexponential function of the kind $Ae^{-t/\tau_A} + Be^{-t/\tau_B}$ is used to fit the decay curve for the ZMWs. Typically, the Ae^{-t/τ_A} term contains information about the fluorescence, whereas Be^{-t/τ_B} is mainly noise. We checked that the contribution of Ae^{-t/τ_A} is at least one magnitude order of larger than that of Be^{-t/τ_B}. Each measurement is repeated several times, and the result is given as the average plus an uncertainty given by the standard deviation.

The lifetime reduction (LR) is measured in two steps. First, the lifetime of the dyes on top of a coverglass is measured (confocal case). Then, the lifetime of the same dyes is measured when they diffuse through the nanoslot (ZMW) in consideration. This gives us the lifetime for the nanoslot case. Then, the lifetime reduction is computed as the lifetime for the confocal case divided by the lifetime for the nanoslot: LR= L_{conf}/L_{ZWM}.

Supporting Note #6 – Gaussian Beam illumination

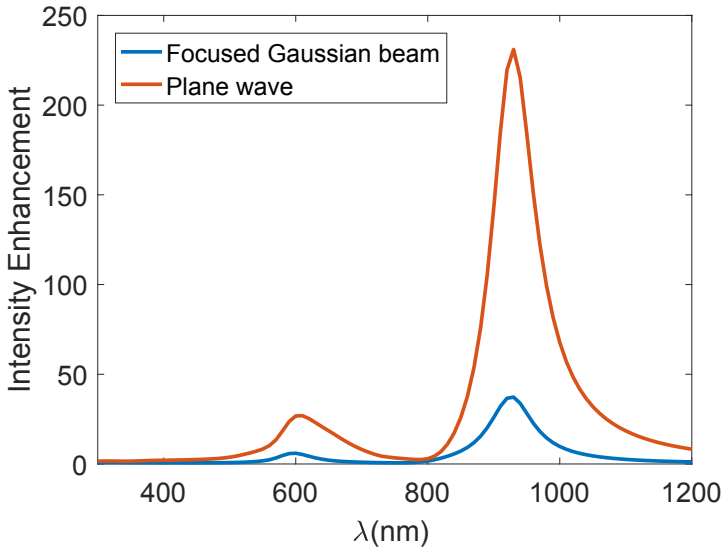

Figure S2: Comparison between the intensity enhancement induced by a tightly focused gaussian beam and a plane-wave.

Supporting References

1s. M. Horák, et al. Comparative study of plasmonic antennas fabricated by electron beam and focused ion beam lithography. *Sci. Rep.* 2018, **8**: 9640.

2s. M. W. Knight, et al. Gallium Plasmonics: Deep Subwavelength Spectroscopic Imaging of Single and Interacting Gallium Nanoparticles. ACS Nano 2015, **9**, 2049-2060.

3s. J. Mao, et al. Effect of Ga Implantation and Hole Geometry on Light Transmission through Nanohole Arrays in Al and Mg. J. Phys. Chem. C 2018, **122**, 10535-10544.

4s. M. Baibakov, S. Patra, J.-B. Claude, A. Moreau, J. Lumeau, J. Wenger, Extending Single-Molecule Förster Resonance Energy Transfer (FRET) Range beyond 10 Nanometers in Zero-Mode Waveguides. *ACS Nano* 2019, DOI: 10.1021/acsnano.9b04378.

5s. T. Miyake, et al. Real-Time Imaging of Single-Molecule Fluorescence with a Zero-Mode Waveguide for the Analysis of Protein-Protein Interaction. *Anal. Chem.* 2008, **80**, 6018–6022.

6s. M. Wu, et al. Fluorescence enhancement in an over-etched gold zero-mode waveguide. *Opt. Exp.* 2019, **27**, 19002-19018.

7s. O. Krichevsky, G. Bonnet, Fluorescence correlation spectroscopy: the technique and its applications. Rep. Prog. Phys 2002, 65, 251–297.

8s. L. Lanzanò, et al. Measurement of nanoscale three-dimensional diffusion in the interior of living cells by STED-FCS. Nat. Commun. 2017, 8, 1–9.